

# Solid–solvent molecular interactions observed in crystal structures of $\beta$ -chitin complexes

Daisuke Sawada · Yu Ogawa · Satoshi Kimura ·  
Yoshiharu Nishiyama · Paul Langan ·  
Masahisa Wada

Received: 24 May 2013 / Accepted: 8 October 2013 / Published online: 15 October 2013  
© Springer Science+Business Media Dordrecht 2013

**Abstract** Three  $\beta$ -chitin structures [anhydrous, dihydrate, mono-ethylenediamine (EDA)] recently determined by synchrotron X-ray and neutron fiber diffraction were reviewed from the viewpoint of molecular interactions. Both water and EDA molecules interact with the chitin chains through multiple hydrogen bonds. When water complexes with chitin, the hydrogen bonding pattern rearranges with the replacement of an intrachain chitin hydrogen bond by a stronger hydrogen bond between chitin and water, with an associated reduction in the degrees of freedom; the water oxygen is a much stronger acceptor than the O5 ring atom. The behavior of hydrogen

exchange by deuterium supports this interpretation. EDA-molecules change the conformation of hydroxymethyl group from *gg* to *gt*, accompanied by changes in hydrogen bonds due to the strong accepting ability of the EDA nitrogen atoms. Some important interactions are in common with experimental crystallographic results of cellulosic crystals and of molecular dynamics studies. These new insights into solid–solvent interactions are valuable in understanding molecular interactions in other polysaccharides-solvents system in solution or on surface.

**Keywords** Structure analysis ·  $\beta$ -chitin · Crystallosolvates · Molecular interaction · Hydrogen bond · Hydroxymethyl group

D. Sawada (✉) · P. Langan  
Biology and Soft Matter Division, Oak Ridge National  
Laboratory, Oak Ridge, TN 37831, USA  
e-mail: sawadad@ornl.gov

Y. Ogawa · S. Kimura · M. Wada  
Department of Biomaterials Science, Graduate School of  
Agricultural and Life Sciences, The University of Tokyo,  
Tokyo 113-8657, Japan

S. Kimura · M. Wada  
Department of Plant and Environmental New Resources,  
College of Life Sciences, Kyung Hee University, 1,  
Seocheon-dong, Giheung-ku, Yongin-si, Gyeonggi-do  
446-701, Republic of Korea

Y. Nishiyama  
Centre de Recherches sur les Macromolécules Végétales  
(CNRS), Affiliated with the Joseph Fourier University of  
Grenoble, BP 53, 38041 Grenoble Cedex 9, France

## Introduction

Chitin, composed of  $\beta$ -1,4 linked 2-acetamide-2-deoxy-D-glucan, is the second most abundant biopolymer on earth after cellulose. While crystalline fibers of cellulose, in association with a matrix of lignin and hemicellulose, play a structural role in plant cell walls, those of chitin, in association with a matrix of proteins, play a similar role in organisms e.g., in the protective shells of arthropods and vestimentiferan tube worms. The structures of cellulose and chitin have been studied extensively since the early twentieth

century. The molecular structure of chitin is similar to that of cellulose except for the replacement of an hydroxyl group by an acetamide group at the C2 position. This acetamide group provides chitin with some unique properties such as biocompatibility (Jayakumar et al. 2010). It also allows chitin to adopt crystalline structures that are different from those available to cellulose.

Chitin chains form molecular sheets through hydrophobic stacking of their glucosamine rings and through  $\text{N-H}\cdots\text{O}=\text{C}$  hydrogen bonds (H-bonds) between the acetamide groups. Chitin has been observed in two major crystalline forms, namely  $\alpha$ -chitin and  $\beta$ -chitin, which produce distinct X-ray and neutron diffraction patterns and infrared and NMR spectra (Rudall 1963; Chanzy et al. 1987; Tanner et al. 1990). The chains in the molecular sheets of  $\alpha$ -chitin have been proposed to pack in an anti-parallel manner, stabilized by intra-sheet H-bonds (Minke and Blackwell 1978). Between the sheets there are also H-bonds. On the other hand the chains in the molecular sheets in  $\beta$ -chitin are parallel (Gardner and Blackwell 1975) with intra-sheet H-bonds but no H-bonding between the sheets. The lack of intersheet H-bonds allows  $\beta$ -chitin to easily incorporate various small polar molecules between the neighboring molecular sheets to form crystalline complexes. Structural information has been provided by X-ray diffraction, electron diffraction, FT-IR and solid state NMR studies for relatively important reagents such as water, alcohols and amines (Blackwell 1969; Kobayashi et al. 2010; Noishiki et al. 2005, 2004, 2003; Saito et al. 2002, 2000; Tanner et al. 1990). Carboxylic anhydride can be incorporated and O6 regioselectively esterified by simple heating (Yoshifuji et al. 2006). How small molecules are trapped and interact with the chitin chains is still unclear, due to the lack of detailed structural information on the complexes at an atomic level.

Over the past 15 years detailed crystal structures of various cellulose and chitin allomorphs, and the complexes of cellulose and chitin with small molecules, have been determined using a combination of high-resolution X-ray and neutron fiber diffraction and computational simulations (Langan et al. 2001, 1999; Nishiyama et al. 2011, 2008, 2003, 2002; Sawada et al. 2013, 2012a, b; Sikorski et al. 2009; Wada et al. 2011, 2009, 2006, 2004). In those studies X-rays were used to provide precise atomic coordinates and thermal

factors for carbon (C), oxygen (O) and nitrogen (N) atoms, and neutrons were then used to locate hydrogen (H) atoms which had been replaced by deuterium (D) atoms. Some of the H atoms in these structures were found to be mobile, or in locations that were not expected from the position of C, O and N atoms in the X-ray structures. Computational simulations were used to interpret disorder, particularly of mobile labile H atoms, and they revealed dynamic trends even for H atoms involved in H-bonds. Other experimental techniques have provided important complementary information on the structure and solid state properties of chitin (Ogawa et al. 2011a, b, 2010). In this paper, we review and examine the wealth of new structural information from the X-ray and neutron structures of anhydrous  $\beta$ -chitin (Nishiyama et al. 2011; Sawada et al. 2012a) di-hydrate  $\beta$ -chitin (Sawada et al. 2012b), and mono-ethylenediamine (EDA)  $\beta$ -chitin (Sawada et al. 2013) and derive some insights that can be used to explain the nature of the actions of amine and solvent molecules on the structure and properties of chitin.

## Materials and methods

### Sample preparation

Satsuma tubeworms (*Lamellibrachia satsuma*) were collected from the sea off Kagoshima Bay at a depth of about 100 m using a remotely operated vehicle, Hyper-Dolphin (JAMSTEC, Japan). The tubes composed of highly crystalline  $\beta$ -chitin and proteins were purified and oriented for fiber diffraction experiment as described previously (Kobayashi et al. 2010). Intracrystalline deuteration of chitin was carried out with hydrothermal treatment in liquid  $\text{D}_2\text{O}$ . The oriented chitin samples were annealed in  $\text{D}_2\text{O}$  for 60 min at 160 °C for neutron diffraction measurement. Thin layer chitin specimens peeled off from the purified tube were also treated in the same solution at various temperatures, ranging from 25 °C to 260 °C to investigate the exchange of H by D with FT-IR spectroscopy.

### FTIR spectroscopy

Exchange of H by D in the crystalline region of chitin was detected by infrared spectroscopy. FT-IR spectra

of chitin samples were recorded with  $4\text{ cm}^{-1}$  resolution and 64 scans on a FT-IR spectrometer, Nicolet Magna 860 (Madison, WI, USA) in transmission mode, and analyzed with OMNIC software (Thermo scientific, Waltham, MA, USA). The spectra were normalized using the  $2,900\text{ cm}^{-1}$  band in the C–H stretching region as an internal standard.

### X-ray data collection

Synchrotron X-ray fiber diffraction data were collected at BL38B1 ( $\lambda = 1.0\text{ \AA}$ ) and BL40B2 ( $\lambda = 0.7\text{ \AA}$ ), at SPring-8, Hyogo Japan. Fiber diffraction patterns were recorded using a flat imaging plate (IP) (Rigaku) from samples of anhydrous, di-hydrate and mono-EDA  $\beta$ -chitin. Data were successfully collected with resolutions up to  $1.0\text{--}1.2\text{ \AA}$ . The maximum resolution depended on the amount of sample and background scattering from solvent. Data were processed as previously described (Nishiyama et al. 2011).

### Neutron data collection

Neutron crystallographic data were collected on diffractometer D19 at the Institut Laue-Langevin, Grenoble France, ( $\lambda = 1.463\text{ \AA}$ ; circular beam cross section of  $8\text{ mm}$  diameter; detector to sample distance of  $761.3\text{ mm}$ ) from a number of capillaries that had been assembled and then glued together to form a  $2\text{ cm} \times 1\text{ cm} \times 2\text{ mm}$  array in order to best exploit the relatively weak flux of the neutron beam. Neutron data were collected from samples of anhydrous and di-hydrate  $\beta$ -chitin; mono-EDA  $\beta$ -chitin has yet to be measured using neutrons. Generic strategies for collecting and processing fiber diffraction data from fibers on D19 have been previously described (Langan et al. 1996; Nishiyama et al. 2008; Sawada et al. 2012a).

### Structure refinement

Structure determination was carried out using previously described strategies for applying *SHELX-97* (Sheldrick 1997) to fiber diffraction data to minimize  $R$ , defined as  $\Sigma(|F_o| - |F_c|)/\Sigma|F_o|$  with  $F_o > 4\sigma$ , where  $F_o$  and  $F_c$  are the observed and calculated structure factor amplitudes respectively (Langan et al. 2001). Labile atom positions (X-ray: hydroxymethyl O6 atom,

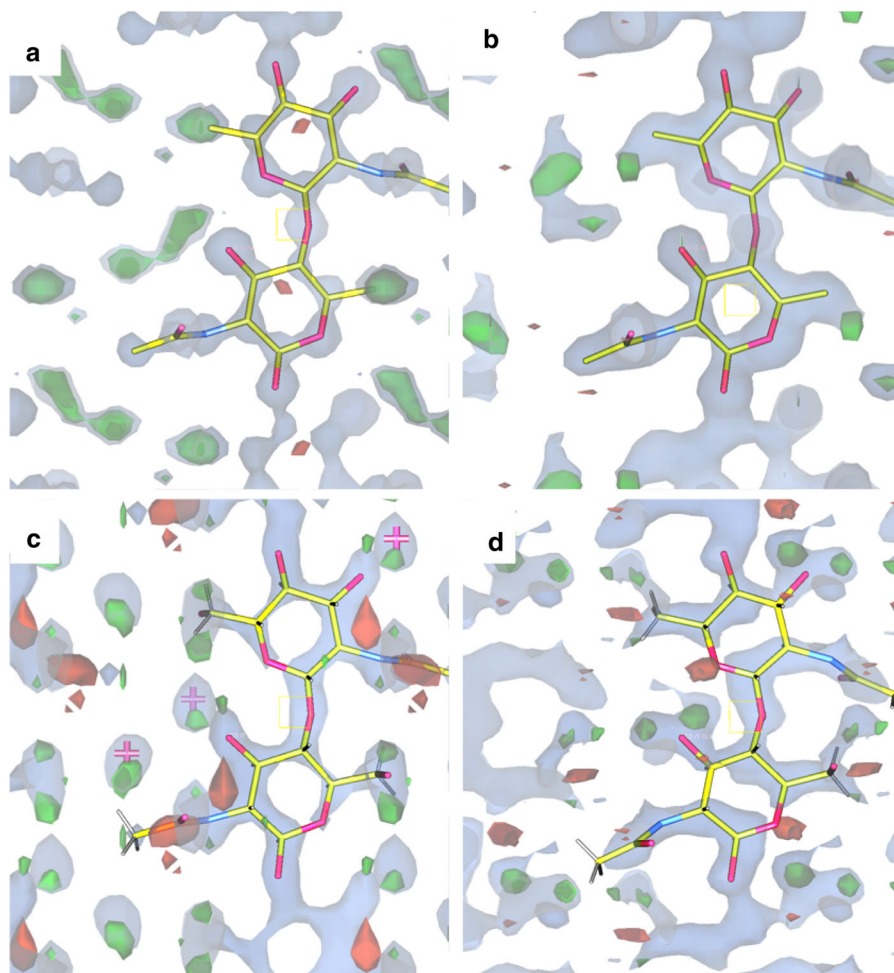
complexed atoms. Neutron: H atoms) were directly located from Fourier omit maps. Calculated  $\sigma_A$  and  $F_o - F_c$  Fourier omit maps were inspected using *Coot* (Emsley and Cowtan 2004). For the further structure refinement, the intensities on the same layer line that were close enough to overlap were grouped. Finally, intensities with very small  $F_c/F_{cmax}$  value were omitted as described previously (Langan et al. 2001).

Recent advances in sample preparation, and fiber diffraction methods, now allow the location of the atomic positions of labile localized H atoms with a high level of confidence. Further, more accurate atomic information including coordinates and thermal displacement factors can be calculated with fewer restraints.

## Results and discussion

The high crystallinity and orientation of the samples of  $\beta$ -chitin complexes used in our studies provided neutron and X-ray diffraction data of high enough quality and resolution to allow the direct location of atoms that were missing in our starting structures. These atoms were visualized in Fourier omit maps, as illustrated in Fig. 1. In this way Fourier maps calculated from X-ray data allowed the location of solvent molecule O, C, and N atoms, and confirmed the conformation of the hydroxymethyl groups, and Fourier maps calculated from neutron data allowed the location of H (as its isotope D) atoms. Surprisingly, we found that density associated with some H positions consisted of more than one peak, and therefore position. This situation has been observed before in neutron structure analyses of cellulose complexes (Wada et al. 2011) and it was interpreted in those studies by using molecular dynamics simulations. Those simulations revealed dynamic trends for H atoms, even when the H atoms were involved in H-bonds, which were consistent with mobility and partial occupancy. The additional scattering density peaks in the  $\beta$ -chitin complexes can also be explained by such dynamic trends. This was not anticipated from the H-bond geometries for putative donor and acceptor atoms in the X-ray structures. Further computational studies will be required to understand the detailed nature of H-bond disorder in chitin and the exact structural properties derived from molecular interactions.

**Fig. 1** Section through the X-ray  $\sigma_A$  (showing positive density in gray) and  $F_o - F_c$  Fourier omit map (showing positive and negative density in green and red). **a:** X-ray di-hydrate **b:** X-ray mono-EDA **c:** Neutron di-hydrate **d:** Neutron anhydrous. Positive density peaks in X-ray map indicated the C, O and N coordinates. Positive density peaks around O and N in neutron map indicated H locations



$\beta$ -chitin can easily incorporate various polar molecules by simple immersion into liquids or solutions. All of the  $\beta$ -chitin complexes we studied could be indexed with a monoclinic unit cell with  $P2_1$  space group symmetry, showing greatest variation in the  $b$ -axis parameter, Table 1. Other  $\beta$ -chitin complexes have been reported that do not have a  $P2_1$  space group due to incompatible stoichiometries between chitin and solvent molecules (Noishiki et al. 2003). The spacing between molecular sheets ( $b$ -axis) expands with the increasing size of guest molecules. The stacking distance ( $a$ -axis) between chains within sheets is reduced in the EDA complex because of the different conformation of the O6 group; the conformation is  $gg$  (perpendicular to ring) in anhydrous  $\beta$ -chitin and the di-hydrate  $\beta$ -chitin complex and  $gt$  (in the plane of the ring) in the EDA  $\beta$ -chitin complex. The experimental unit cell volumes of anhydrous, di-hydrate and mono-EDA  $\beta$ -

chitin are  $459.4 \text{ \AA}^3$ ,  $556.8 \text{ \AA}^3$ , and  $686.30 \text{ \AA}^3$ , respectively. Interestingly, if we take the unit cell volume of anhydrous  $\beta$ -chitin and add the bulk liquid volumes of water and EDA solvent molecules we get values of  $579 \text{ \AA}^3$  and  $681.4 \text{ \AA}^3$  for di-hydrate and mono-EDA  $\beta$ -chitin. The significantly smaller experimental value for di-hydrate  $\beta$ -chitin suggests that water molecules are more strongly bound in the complex. On the other hand, the larger experimental value for mono-EDA  $\beta$ -chitin suggests that the EDA molecules are less confined and restrained in the complex. These results are consistent with the crystallographically determined (di-hydrate) and predicted (EDA) H-bonding systems. Water molecules are localized in an H-bonding network in the di-hydrate  $\beta$ -chitin structure. On the contrary, one of the nitrogen atoms must be completely free from the H-bonding from the geometric prediction of EDA complex structure.

**Table 1** Crystal information of  $\beta$ -chitin X-ray structures

	a (Å)	b (Å)	c (Å)	$\gamma$ (°)	V (Å <sup>3</sup> )	O6
Anhydrous	4.820 (3)	9.247 (4)	10.390 (5)	97.21 (7)	459.4	<i>gg</i>
Di-hydrate	4.814 (5)	11.167 (9)	10.423 (10)	96.45 (5)	556.8	<i>gg</i>
Mono-EDA	4.682 (4)	14.351 (4)	10.275 (6)	96.24 (5)	686.3	<i>gt</i>

An important observation from the structural analysis of the di-hydrate  $\beta$ -chitin structure (Fig. 2a) was the absence of an intramolecular H-bond between hydroxyl group O3 and ring oxygen O5. Instead, O3 donates H in an H-bond to a water O atom. The slightly, but importantly, bigger repeating distance (*c*-axis) of di-hydrate  $\beta$ -chitin is consistent with a relaxation along the chain direction due to the absence of this intramolecular H-bond (Table 1). The twofold symmetry of chitin and cellulose chains produces a close distance between O3 and O5 and an O3–O5 intramolecular H-bond has been observed in almost all crystal structures of cellulose allomorphs and cellulosic small molecules (French and Jonson 2004). It would appear that a favorable distance between O3 and O5 is not sufficient for creation of an intrachain O3–O5 H-bond if there is another stronger acceptor near O3. This result demonstrates the importance of using neutron diffraction in addition to X-ray diffraction in order to provide direct information about the location of H atoms. Interestingly, the absence of this H-bond agrees with molecular dynamics studies of cellulose. O3 of cellulose oligomers in aqueous solution (Shen et al. 2009) or of hydrated cellulose surfaces (Chundawat et al. 2011) preferentially H-bond with water rather than O5. The relatively free solvent molecules in  $\beta$ -chitin complexes have the ability to exhibit some features of interactions between hydroxyl groups and solvent molecules. Interestingly, the O6 group of  $\beta$ -chitin takes the *gg* conformation when interacting with water molecules in di-hydrate  $\beta$ -chitin which is also observed when at the aqueous surfaces of cellulose II hydrate (Kobayashi et al. 2011) and in cellulose oligomers in aqueous solution (Shen et al. 2009).  $\beta$ -chitin is known to form another water complex, monohydrate, having a water molecule per a GlcNAc residue (Blackwell 1969). Because a well-aligned H-bonding system in di-hydrate  $\beta$ -chitin is established by appropriate positioning of two water molecules, the loss of one water molecule implies the collapse of the H-bonding system. A solid-state NMR study (Kobayashi et al. 2010) indicated that the mono-

hydrate structure is a mixture of the di-hydrate and anhydrous structure. Some O3–O5 H-bonds may therefore be reformed in the mono-hydrate structure.

Further information on the nature of H-bonding can be obtained by considering the extent to which H atoms are replaced by D atoms, which can be obtained by refining the occupancies at these positions (Ogawa et al. 2012). When di-hydrate  $\beta$ -chitin is simply immersed in heavy water at room temperature there is a difference in the partial intracrystalline deuteration of the functional groups; the D/H ratio is 25 % for the O3 and O6 atoms and it is even less for the N–H groups. One explanation for this is that the two hydroxyl groups have direct H-bonds with water molecules and can therefore be more easily exchanged, whereas N–H groups do not interact directly with water molecules but only with the adjacent chitin molecules and are therefore more protected. Direct interactions with water would appear to induce D/H exchange but complete deuteration does not occur. When samples are hydrothermally treated in heavy water the exchange is more extensive and rapid. Almost all the H atoms on O3 and at least half of the H atoms on amine groups are exchanged by D with treatment at 80 °C. The preferential exchange on O3 could be explained by the H-bonding network. Since water in the complex H-bonds to O3 with the closest donor-acceptor distance observed in the structure, the exchange between D and H occurs frequently at high temperatures. In addition, O3 participates in an extended H-bond network by donating H in an H-bond to a water molecule, not to ring oxygen O5. The extended cooperative H-bond network along the *a*-axis direction probably runs along the length of crystalline domains, and it might help the deuteration of the O3 hydroxyl groups. Almost all crystals of cellulose, chitin, and their complexes that we have studied so far have this type of cooperative H-bond network, and it would appear to influence the intracrystalline susceptibility of H atoms to exchange by D. In general, however, the degree of crystallinity is also important e.g., exchange of H by D in highly crystalline cellulose is limited



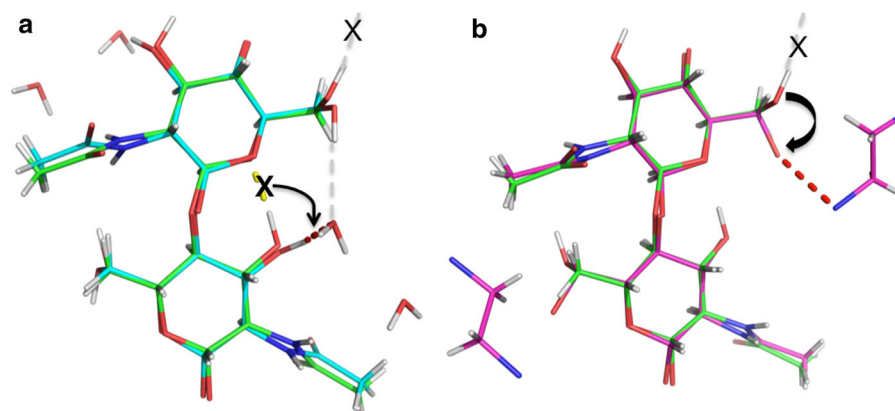


**Fig. 2** Characteristic crystalline transition from anhydrous structure (green backbone) with the water (a; blue backbone) and EDA (b; purple backbone) molecule

(Nishiyama et al. 1999) whereas in wood pulp cellulose the majority of hydroxyl groups are exchanged (Frilette et al. 1948).

Amines can penetrate into both cellulose and chitin crystals. Some amines with various salts can dissolve cellulose completely (Xiao and Frey 2007). They can also convert naturally occurring cellulose from cellulose I to more activated cellulose III<sub>I</sub> (Chanzy et al. 1987; Igarashi et al. 2007; Wada et al. 2001). Thus, molecular interactions between glucans and amines are of great interest because they should relate to the driving force transforming cellulose crystals. A combined study of X-ray fiber diffraction, neutron fiber diffraction and computational calculations has been carried out for the ammonia-cellulose I complex (Wada et al. 2004, 2011), and a high-resolution X-ray structure was reported for the EDA-cellulose I complex (Wada et al. 2009). The hydroxymethyl group O6 takes the *gt* conformation in both of the ammonia and EDA complex structures. In the study of ammonia-cellulose I, N atoms of ammonia accept well-occupied H-bonds especially from O6. This strong accepting capability of ammonia may be the driving force needed to break the H-bond pattern in cellulose I and then to rotate the O6 from *tg*, which is energetically unfavorable in solution, to *gt*, as the ammonia-cellulose complex is formed. This strong accepting capability of nitrogen can be observed in the EDA-cellulose I complex. In the mono-EDA  $\beta$ -chitin structure (Fig. 2b), this feature is more emphasized because EDA molecules in  $\beta$ -chitin have a larger free volume to move within the crystals as described above. The N atom of EDA can accept a very strong

H-bond from O6 (2.54 Å). The hydroxymethyl O6 is also rotated to the *gt* conformation from the (almost same energy) *gg* conformation. The *gt* conformation allows O3 and O6 hydroxyl group to form an O3–O6 intramolecular H-bond. The significantly smaller repeating distance (c-axis) of the mono-EDA structure (Table 1) is probably due to these H bonds being biased to one side of glycosidic bond around O3, O6 and N (of EDA).

## Conclusion

The detailed crystal information of  $\beta$ -chitin complexes from high-resolution X-ray and neutron fiber diffraction studies provides a wealth of new information on the interaction of chitin with solvents. The complexed molecules (water, EDA) interact with chitin side groups and change the chitin conformation and H-bonding systems. The common effect of water and EDA is to disrupt the O3–O5 intramolecular H-bond and change the conformation of the hydroxymethyl O6 group. These results suggest how solvent molecules may interact with the surfaces of chitin fibers and therefore may be useful in understanding the detailed action of solvents on polysaccharides and on different types of biomass during its industrial processing.

**Acknowledgments** We thank beamline D19 at the Institut Laue-Langevin, BL38B1 and BL40B2 at SPring-8 for use of facilities. We thank the Japan Agency for Marine–Earth Science and Technology (JAMSTEC) for collecting samples of *L. satsuma* using a remotely operated vehicle, Hyper-Dolphin. PL was partly supported by Genomic Science Program, Office of Biological and Environmental Research, US Department of

Energy, under FWP ERKP752 and the US Department of Energy, managed by UT-Battelle, LLC under contract No. DE-AC05-00OR22725. PL acknowledges support by the Scientific User Facilities Division, Office of Basic Energy Sciences. YO was supported by grant-in-aids for JSPS research fellow (23-2362).

## References

- Blackwell J (1969) Structure of  $\beta$ -chitin or parallel chain systems of poly- $\beta$ -(1  $\rightarrow$  4)-N-acetyl-D-glucosamine. *Biopolymers* 7:281–298. doi:[10.1002/bip.1969.360070302](https://doi.org/10.1002/bip.1969.360070302)
- Chanzy H, Henrissat B, Vincendon M et al (1987) Solid-state  $^{13}\text{C}$ -N.M.R. and electron microscopy study on the reversible cellulose I  $\rightarrow$  cellulose III<sub>I</sub> transformation in Valonia. *Carbohydr Res* 160:1–11. doi:[10.1016/0008-6215\(87\)80299-9](https://doi.org/10.1016/0008-6215(87)80299-9)
- Chundawat SPS, Bellesia G, Uppugundla N et al (2011) Restructuring the crystalline cellulose hydrogen bond network enhances its depolymerization rate. *J Am Chem Soc* 133:11163–11174. doi:[10.1021/ja2011115](https://doi.org/10.1021/ja2011115)
- Emsley P, Cowtan K (2004) Coot: model-building tools for molecular graphics. *Acta Crystallogr D Biol Crystallogr* 60:2126–2132. doi:[10.1107/S0907444904019158](https://doi.org/10.1107/S0907444904019158)
- French AD, Johnson GP (2004) What crystals of small analogs are trying to tell us about cellulose structure. *Cellulose* 11:5–22
- Frilette VJ, Hanle J, Mark H (1948) Rate of exchange of cellulose with heavy water. *J Am Chem Soc* 70:1107–1113
- Gardner KH, Blackwell J (1975) Refinement of the structure of  $\beta$ -chitin. *Biopolymers* 14:1581–1595. doi:[10.1002/bip.1975.360140804](https://doi.org/10.1002/bip.1975.360140804)
- Igarashi K, Wada M, Samejima M (2007) Activation of crystalline cellulose to cellulose III<sub>I</sub> results in efficient hydrolysis by cellobiohydrolase. *FEBS J* 274:1785–1792. doi:[10.1111/j.1742-4658.2007.05727.x](https://doi.org/10.1111/j.1742-4658.2007.05727.x)
- Jayakumar R, Menon D, Manzoor K et al (2010) Biomedical applications of chitin and chitosan based nanomaterials—A short review. *Carbohydr Polym* 82:227–232. doi:[10.1016/j.carbpol.2010.04.074](https://doi.org/10.1016/j.carbpol.2010.04.074)
- Kobayashi K, Kimura S, Togawa E, Wada M (2010) Crystal transition between hydrate and anhydrous  $\beta$ -chitin monitored by synchrotron X-ray fiber diffraction. *Carbohydr Polym* 79:882–889. doi:[10.1016/j.carbpol.2009.10.020](https://doi.org/10.1016/j.carbpol.2009.10.020)
- Kobayashi K, Kimura S, Togawa E, Wada M (2011) Crystal transition from cellulose II hydrate to cellulose II. *Carbohydr Polym* 86:975–981. doi:[10.1016/j.carbpol.2011.05.050](https://doi.org/10.1016/j.carbpol.2011.05.050)
- Langan P, Denny RC, Mahendrasingam A et al (1996) Collecting and processing neutron fibre diffraction data from a single-crystal diffractometer. *J Appl Crystallogr* 29:383–389. doi:[10.1107/S0021889896002816](https://doi.org/10.1107/S0021889896002816)
- Langan P, Nishiyama Y, Chanzy H (1999) A revised structure and hydrogen-bonding system in cellulose II from a neutron fiber diffraction analysis. *J Am Chem Soc* 121:9940–9946. doi:[10.1021/ja9916254](https://doi.org/10.1021/ja9916254)
- Langan P, Nishiyama Y, Chanzy H (2001) X-ray structure of mercerized cellulose II at 1 Å resolution. *Biomacromolecules* 2:410–416. doi:[10.1021/bm005612q](https://doi.org/10.1021/bm005612q)
- Minke R, Blackwell J (1978) The structure of  $\alpha$ -chitin. *J Mol Biol* 120:167–181. doi:[10.1016/0022-2836\(78\)90063-3](https://doi.org/10.1016/0022-2836(78)90063-3)
- Nishiyama Y, Isogai A, Okano T et al (1999) Intracrystalline deuteration of native cellulose. *Macromolecules* 32:2078–2081. doi:[10.1021/ma981563m](https://doi.org/10.1021/ma981563m)
- Nishiyama Y, Langan P, Chanzy H (2002) Crystal structure and hydrogen-bonding system in cellulose I $\beta$  from synchrotron X-ray and neutron fiber diffraction. *J Am Chem Soc* 124:9074–9082. doi:[10.1021/ja0257319](https://doi.org/10.1021/ja0257319)
- Nishiyama Y, Sugiyama J, Chanzy H, Langan P (2003) Crystal structure and hydrogen bonding system in cellulose I $\alpha$  from synchrotron X-ray and neutron fiber diffraction. *J Am Chem Soc* 125:14300–14306. doi:[10.1021/ja037055w](https://doi.org/10.1021/ja037055w)
- Nishiyama Y, Johnson GP, French AD et al (2008) Neutron crystallography, molecular dynamics, and quantum mechanics studies of the nature of hydrogen bonding in cellulose I $\beta$ . *Biomacromolecules* 9:3133–3140. doi:[10.1021/bm800726v](https://doi.org/10.1021/bm800726v)
- Nishiyama Y, Noishiki Y, Wada M (2011) X-ray structure of anhydrous  $\beta$ -chitin at 1 Å resolution. *Macromolecules* 44:950–957. doi:[10.1021/ma102240r](https://doi.org/10.1021/ma102240r)
- Noishiki Y, Nishiyama Y, Wada M et al (2003) Inclusion complex of  $\beta$ -chitin and aliphatic amines. *Biomacromolecules* 4:944–949. doi:[10.1021/bm034024k](https://doi.org/10.1021/bm034024k)
- Noishiki Y, Kuga S, Wada M et al (2004) Guest selectivity in complexation of  $\beta$ -chitin. *Macromolecules* 37:6839–6842. doi:[10.1021/ma0489265](https://doi.org/10.1021/ma0489265)
- Noishiki Y, Nishiyama Y, Wada M, Kuga S (2005) Complexation of  $\alpha$ -chitin with aliphatic amines. *Biomacromolecules* 6:2362–2364. doi:[10.1021/bm0500446](https://doi.org/10.1021/bm0500446)
- Ogawa Y, Kimura S, Wada M, Kuga S (2010) Crystal analysis and high-resolution imaging of microfibrillar  $\alpha$ -chitin from *Phaeocystis*. *J Struct Biol* 171:111–116. doi:[10.1016/j.jsb.2010.03.010](https://doi.org/10.1016/j.jsb.2010.03.010)
- Ogawa Y, Hori R, Kim U-J, Wada M (2011a) Elastic modulus in the crystalline region and the thermal expansion coefficients of  $\alpha$ -chitin determined using synchrotron radiated X-ray diffraction. *Carbohydr Polym* 83:1213–1217. doi:[10.1016/j.carbpol.2010.09.025](https://doi.org/10.1016/j.carbpol.2010.09.025)
- Ogawa Y, Kimura S, Wada M (2011b) Electron diffraction and high-resolution imaging on highly-crystalline  $\beta$ -chitin microfibril. *J Struct Biol* 176:83–90. doi:[10.1016/j.jsb.2011.07.001](https://doi.org/10.1016/j.jsb.2011.07.001)
- Ogawa Y, Kimura S, Saito Y, Wada M (2012) Infrared study on deuteration of highly-crystalline chitin. *Carbohydr Polym* 90:650–657. doi:[10.1016/j.carbpol.2012.05.092](https://doi.org/10.1016/j.carbpol.2012.05.092)
- Rudall KM (1963) The chitin/protein complexes of insect cuticles. *Adv Insect Physiol* 1:257–313
- Saito Y, Okano T, Gaill F et al (2000) Structural data on the intra-crystalline swelling of  $\beta$ -chitin. *Int J Biol Macromol* 28:81–88. doi:[10.1016/S0141-8130\(00\)00147-1](https://doi.org/10.1016/S0141-8130(00)00147-1)
- Saito Y, Kumagai H, Wada M, Kuga S (2002) Thermally reversible hydration of  $\beta$ -chitin. *Biomacromolecules* 3:407–410. doi:[10.1021/bm015646d](https://doi.org/10.1021/bm015646d)
- Sawada D, Nishiyama Y, Langan P et al (2012a) Water in crystalline fibers of dihydrate  $\beta$ -chitin results in unexpected absence of intramolecular hydrogen bonding. *PLoS ONE* 7:e39376. doi:[10.1371/journal.pone.0039376](https://doi.org/10.1371/journal.pone.0039376)
- Sawada D, Nishiyama Y, Langan P et al (2012b) Direct determination of the hydrogen bonding arrangement in

- anhydrous  $\beta$ -chitin by neutron fiber diffraction. *Biomacromolecules* 13:288–291. doi:[10.1021/bm201512t](https://doi.org/10.1021/bm201512t)
- Sawada D, Kimura S, Nishiyama Y et al (2013) The crystal structure of mono-ethylenediamine  $\beta$ -chitin from synchrotron X-ray fiber diffraction. *Carbohydr Polym* 92:1737–1742. doi:[10.1016/j.carbpol.2012.11.025](https://doi.org/10.1016/j.carbpol.2012.11.025)
- Shen T, Langan P, French AD et al (2009) Conformational flexibility of soluble cellulose oligomers: chain length and temperature dependence. *J Am Chem Soc* 131:14786–14794. doi:[10.1021/ja9034158](https://doi.org/10.1021/ja9034158)
- Sikorski P, Hori R, Wada M (2009) Revisit of  $\alpha$ -chitin crystal structure using high resolution X-ray diffraction data. *Biomacromolecules* 10:1100–1105. doi:[10.1021/bm801251e](https://doi.org/10.1021/bm801251e)
- Tanner SF, Chanzy H, Vincendon M et al (1990) High-resolution solid-state carbon-13 nuclear magnetic resonance study of chitin. *Macromolecules* 23:3576–3583. doi:[10.1021/ma00217a008](https://doi.org/10.1021/ma00217a008)
- Wada M, Heux L, Isogai A et al (2001) Improved structural data of cellulose III<sub>I</sub> prepared in supercritical ammonia. *Macromolecules* 34:1237–1243. doi:[10.1021/ma001406z](https://doi.org/10.1021/ma001406z)
- Wada M, Chanzy H, Nishiyama Y, Langan P (2004) Cellulose III<sub>I</sub> crystal structure and hydrogen bonding by synchrotron X-ray and neutron fiber diffraction. *Macromolecules* 37:8548–8555. doi:[10.1021/ma0485585](https://doi.org/10.1021/ma0485585)
- Wada M, Nishiyama Y, Langan P (2006) X-ray structure of ammonia–cellulose I: new Insights into the conversion of cellulose I to cellulose III<sub>I</sub>. *Macromolecules* 39:2947–2952. doi:[10.1021/ma060228s](https://doi.org/10.1021/ma060228s)
- Wada M, Heux L, Nishiyama Y, Langan P (2009) The structure of the complex of cellulose I with ethylenediamine by X-ray crystallography and cross-polarization/magic angle spinning <sup>13</sup>C nuclear magnetic resonance. *Cellulose* 16:943–957
- Wada M, Nishiyama Y, Bellesia G et al (2011) Neutron crystallographic and molecular dynamics studies of the structure of ammonia–cellulose I: rearrangement of hydrogen bonding during the treatment of cellulose with ammonia. *Cellulose* 18:191–206
- Xiao M, Frey MW (2007) The role of salt on cellulose dissolution in ethylene diamine/salt solvent systems. *Cellulose* 14:225–234
- Yoshifuji A, Noishiki Y, Wada M et al (2006) Esterification of  $\beta$ -chitin via intercalation by carboxylic anhydrides. *Biomacromolecules* 7:2878–2881. doi:[10.1021/bm060516w](https://doi.org/10.1021/bm060516w)